5 FEASIBILITY STUDIES: WAVEFORM INVESTIGATION AND DATA REDUCTION

5.1 Introduction

A series of field trials were performed using the instrumentation and field procedure described in Chapter 4. One of the principal objectives of these trials was to establish that the SAM method was technically feasible. They were designed to provide confirmation of the performance specifications of the transducer as well as an appraisal of signal levels and data quality. In addition, appropriate data reduction procedures were to be developed and tested.

This chapter focuses on the results of the feasibility trials which are relevant to the above objectives. An investigation of the recorded waveforms is described and the data reduction procedures adopted to extract the required information from the recorded data are presented.

5.2 Parameters of the SAM Waveform

The naming conventions defined in Table 5-1 summarise the components of the signal recorded during a SAM survey.

Name	Symbol	Description
Total Magnetic Field (Raw Data)	H_T	The time-varying, total magnetic field intensity waveform recorded during a SAM survey. It consists of two major spectrally distinct components, H_S and H_{Mod}.
Spatially-varying Magnetic Field (TMI)	H_S	The spatially-varying magnetic field - Total Magnetic Intensity (observed as a time-varying magnetic field when the survey is conducted whilst continuously traversing over the ground).
SAM Modulation (SAM Signal)	H_{Mod}	The modulation on H_S due to the transmitted signal. It consists of two major components, $H_{Primary}$ and H_G.
Peak Amplitude of SAM Modulation	H_{Pk}	The peak amplitude of H_{Mod} measured during the transmitter "On" time.
Primary Field	$H_{Primary}$	The magnetic field due to current flowing in the wires from the transmitter.
Ground Field	H_G	The magnetic field due to the artificially induced current flowing through the ground.
Normal Field	H_{Normal}	The magnetic field expected due to the artificially induced current flowing through a homogeneous earth.
Normalised Field	H_N	The Normalised TFMMR anomaly - determined by subtracting $H_{Primary}$ and H_{Normal} from H_{Mod}.

Table 5-1. The naming convention and symbols used to describe the components of the SAM waveform.

Figure 5-1 is a typical 10 s raw data set (H_T) recorded during one of the SAM feasibility trials. These data were sampled by the TM-4 in free run mode at a rate of approximately 200 measurements per second whilst the sensor was moved across the ground at a speed of approximately 1.5 m/s. Consequently, the profile corresponds to 15 m of traverse. The profile readily displays the artificially induced 8 Hz modulation, H_{Mod}, superimposed on the spatially-varying magnetic field, H_S. The signals of interest are H_S and the Ground field, H_G.

A series of data reduction procedures were required to extract these signals from the raw data, H_T. The procedures applied to this feasibility trial data are described in Section 5.4 and are illustrated with examples of actual recorded data.

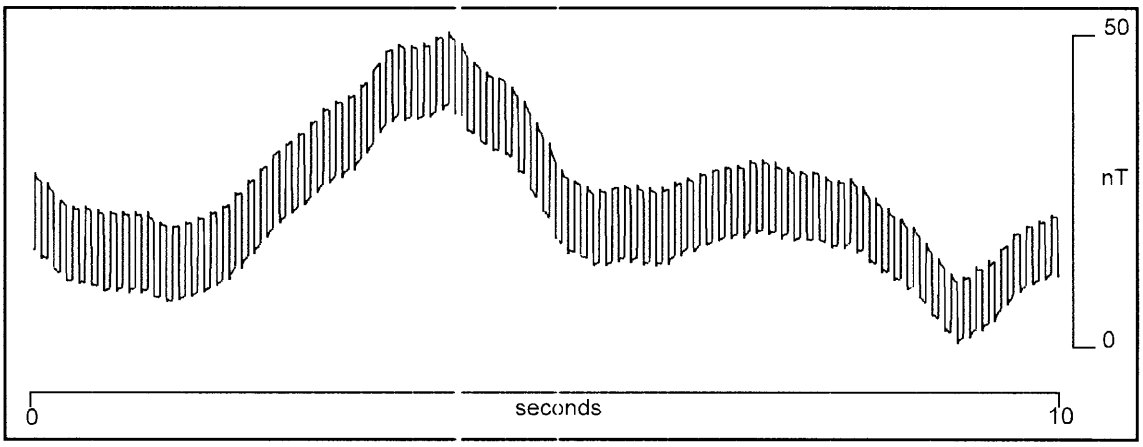

Figure 5-1. A ten second time sample (15 m traverse length) illustrating the artificially induced modulation, H_{Mod}, superimposed on the spatially-varying magnetic field, H_S.

5.3 Investigation of the Recorded Waveforms

In order to understand the data reduction procedures employed to extract the desired information relating to the TFMMR and TFMMIP parameters and to understand the effect of induced polarisation and / or EM coupling on the waveforms, it was first necessary to fully comprehend the physical relationships that determine the character of the recorded waveforms.

5.3.1 Waveform Types

A visual inspection of the recorded waveforms revealed some interesting features. The waveforms showed considerable variation in both amplitude and character. Examples of these are shown in Figure 5-2 and include the following:

(i). **Square wave** - This was the most common waveform type observed in the recorded data. It occurs particularly in areas proximal to the current carrying wire where the received signal is dominated by the Primary field ($H_{Primary}$) (see Figure 5-2(A)).

(ii). **Spikes** - This waveform consists of a series of spikes of alternating polarity, each occurring at the frequency of the fundamental (see Figure 5-2(B)).

(iii). **Square waves with spikes** - In some situations, the observed signal consists of square waves superimposed by spikes at the trailing edge (see Figure 5-2(C)).

(iv). **Amplitude modulation of spikes** - The spikes referred to in (ii) and (iii) vary in amplitude with a consistent pattern indicating amplitude modulation.

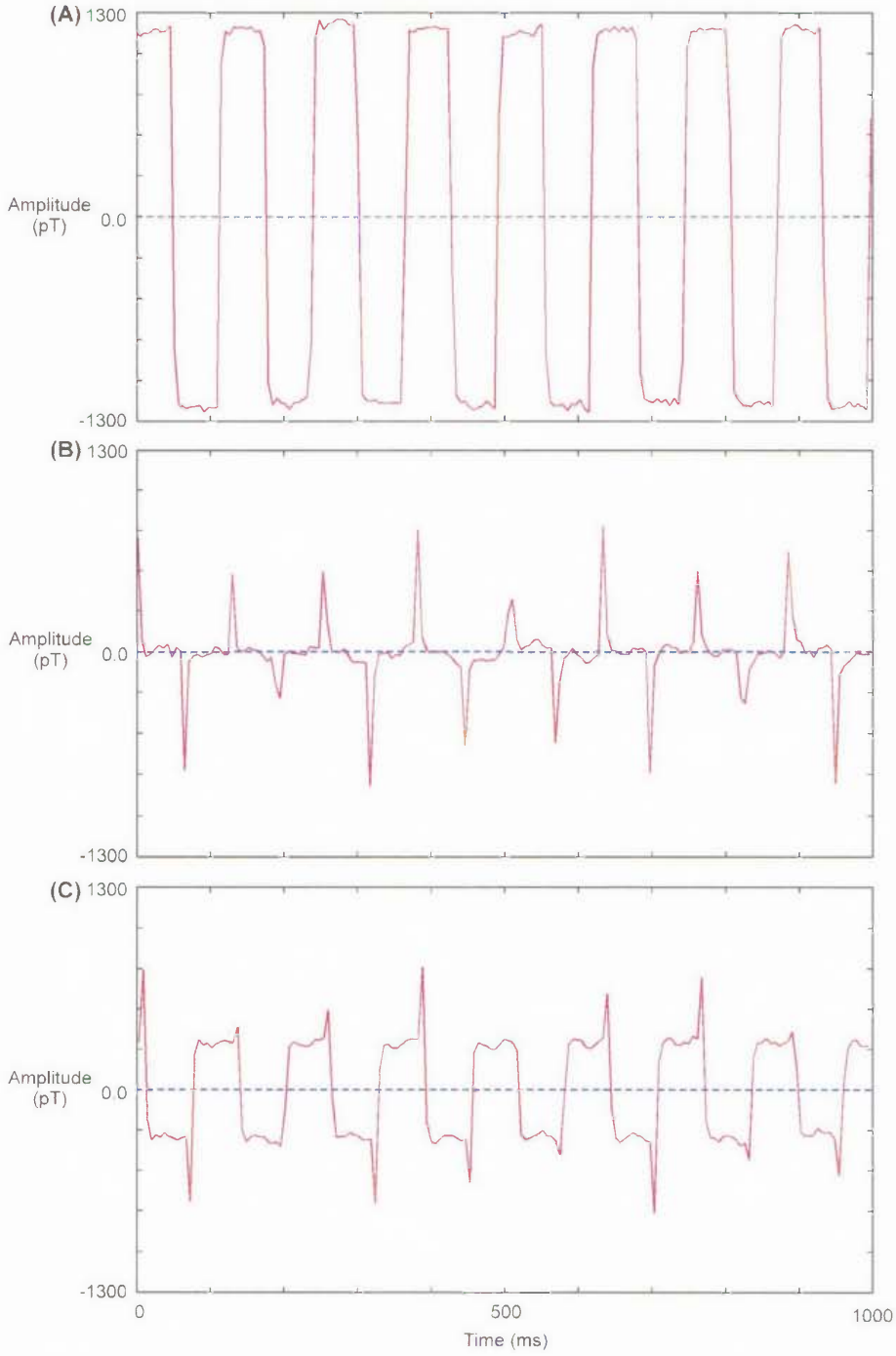

Figure 5-2. Examples of recorded waveforms for a one second time interval. (A) Typical square waves. (B) Spikes. (C) Square waves with spikes.

An understanding of these waveforms was achieved by modelling the effect of the vectorial addition of the signals involved. As defined in Chapter 3, the SAM signal, H_{Mod}, consists of two components, the Primary field, $H_{Primary}$, and the Ground field, H_G. For a given direction of current flow, the polarity of $H_{Primary}$ does not change within the survey area and the amplitude varies inversely with distance from the wire. However, the same cannot be said for H_G which may vary within the survey area in amplitude, polarity and phase with respect to the transmitted current.

5.3.2 The Effect of Superposition of $H_{Primary}$ and H_G

Numerical calculations were performed in order to investigate the effects of amplitude, polarity and phase on the superposition of the spike and square wave profiles that were observed in the real data represented in Figure 5-2. The effects of superposition of in-phase and phase-shifted waveforms are illustrated over a 0.25 s time period for an 8 Hz, 100% duty cycle square wave in Figures 5-3 and 5-4.

5.3.2.1 In-Phase Signals

Figure 5-3(A) illustrates the effect of adding a 10 nT Primary field ($H_{Primary}$) to a 5 nT Ground field (H_G) both of which are of the same polarity. $H_{Primary}$ and H_G are in phase. The resultant is a 15 nT square wave. If $H_{Primary}$ and H_G are equal in amplitude, in phase but of opposite polarity (or more correctly, 180° out-of-phase), the resultant waveform will be a null signal as shown in Figure 5-3(B). Where H_G is larger in amplitude than $H_{Primary}$, in-phase but of opposite polarity, as shown in Figure 5-3(C), the resultant signal will be of the same polarity as H_G but reduced in amplitude by an amount equal to the amplitude of $H_{Primary}$.

It can be seen, therefore, that variation along a profile in both the relative amplitude and polarities of $H_{Primary}$ and H_G may result in the "pinching out" of the amplitude of the resultant signal at the point of polarity reversal. In none of these resultant waveforms do the previously mentioned spikes occur. Each of these resultant waveforms can be observed in real data.

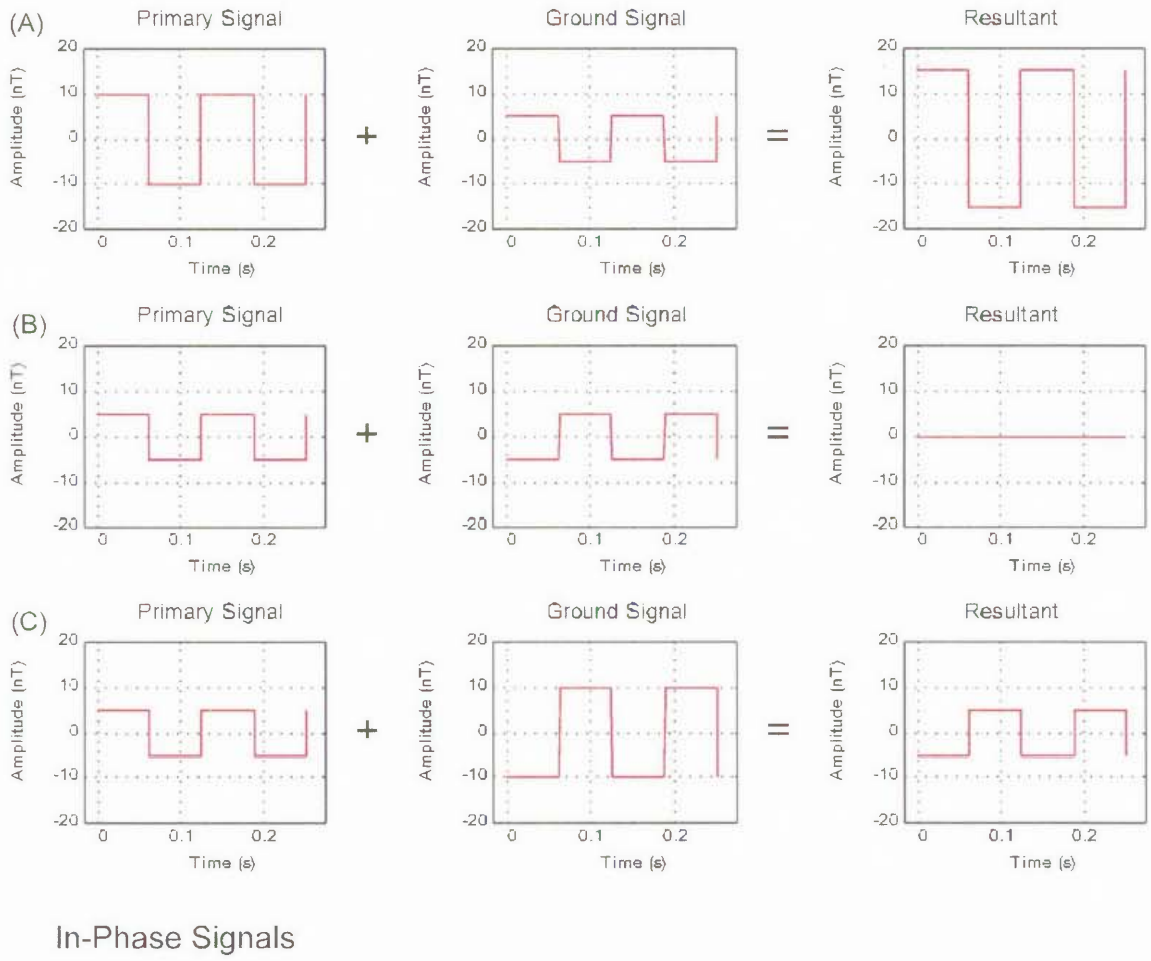

Figure 5-3. The effect of superposition of $H_{Primary}$ and H_G (8 Hz, 100% duty cycle) for in-phase signals.

5.3.2.2 Out-Of-Phase Signals

The presence of induced polarisation and / or electromagnetic induction will introduce a phase lag in H_G with respect to $H_{Primary}$. The effect of this phase lag on the shape and character of the resultant waveform is illustrated in Figure 5-4. For the purpose of discussion, a 50 mrad phase lag has been introduced into H_G. Where $H_{Primary}$ and H_G are of the same polarity, the resultant waveform will be a slightly distorted square wave of amplitude equal to the sum of the amplitudes of $H_{Primary}$ and H_G (see Figure 5-4(A)).

If $H_{Primary}$ and H_G are of equal amplitude, but of opposite polarity, then the combined signals will effectively null at all points except where the signals don't overlap. The resultant signal is, therefore, a series of positive and negative spikes each occurring at a frequency equivalent to that of the transmitted frequency Figure 5-4(B) and of width equal to the phase lag.

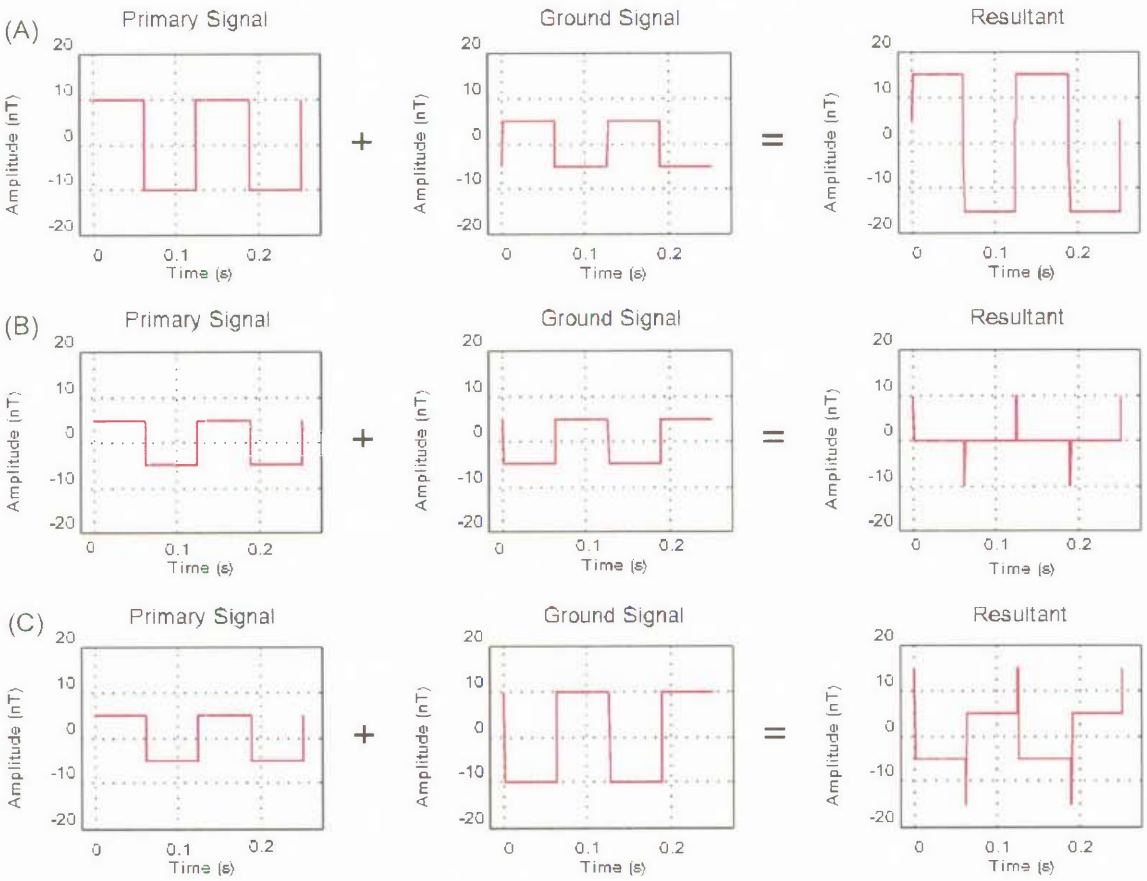

Figure 5-4. The effect of superposition of $H_{Primary}$ and H_G (8 Hz, 100% duty cycle) with a phase lag of 50 mrad.

Where H_G is larger in amplitude than $H_{Primary}$ and opposite in polarity as shown in Figure 5-4(C), the resultant waveform will be a square wave of the same polarity as H_G but of reduced amplitude, with spikes occurring again at the points where the two signals don't completely overlap.

The apparent modulation of the amplitude of the spikes is due to the effect of sampling the magnetic field at a rate which is not a multiple of the transmitter frequency, causing the sampling points to fall at varying points along the waveforms.

As with the synthetic in-phase data, each of these waveforms may also be encountered in real data where this data contains a phase shift due to induced polarisation and / or electromagnetic coupling. These simulations confirm that the spikes sometimes observed in real data are a consequence of an understood phenomenon and are not an artefact of the operation of the transmitter or magnetometer instrumentation.

5.4 Data Reduction Procedures

The receiver instrumentation used to demonstrate the SAM concept lacked synchronisation with the transmitter. This deficiency, together with the non-constant sample interval typical of the period counter in the TM-4, meant that the use of conventional IP data processing techniques such as stacking and integration to determine TFMMR and TFMMIP parameters was not possible. The non-conventional approach used for the trials are described as follows:

5.4.1 Extraction of H_S and H_{Mod} from H_T

Figure 5-5(A) is an example of H_T for a single traverse across a conductor. As can be seen from the figure, the artificially induced modulation, H_{Mod}, is readily visible. The initial step in the data processing procedure was to obtain H_S, by applying a lowpass, 6th order, zero-phase Butterworth Filter using a cutoff frequency of 5 Hz. Subtraction of H_S from H_T then extracts the SAM signal, H_{Mod}. The three waveforms are each depicted in Figure 5-5.

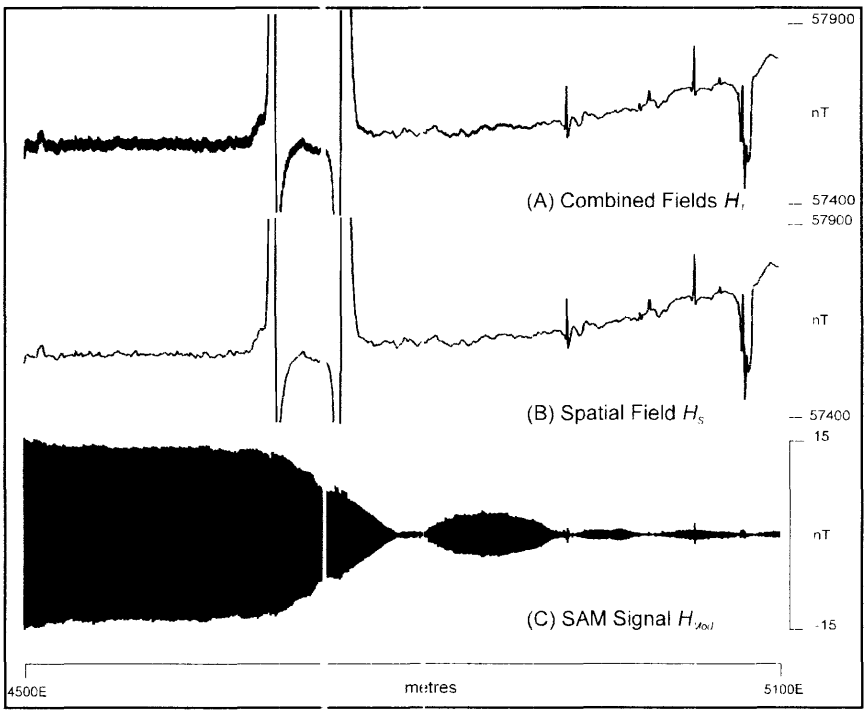

Figure 5-5. (A) A sample raw data profile H_T recorded over a conductor. The component signals were separated by digital filtering to produce: (B) The spatially-varying magnetic field data H_S, and (C) The SAM signal H_{Mod}.

In this example, the current wires were laid out to the west of the survey area. The high amplitude modulation at the western end of the profile is dominated by the influence of the Primary magnetic field ($H_{Primary}$) due to current flowing in these wires. Note also the variation in the SAM signal (H_{Mod}) envelope along the profile.

5.4.2 Correction of H_S for Temporal Variation

The spatial field (H_S) data were resampled at 0.5 m intervals and corrected for diurnal variation by subtracting the data recorded with a synchronised base-station magnetometer as per a conventional magnetometer survey.

5.4.3 Extraction of TFMMR Information

The TFMMR information is contained in the amplitude of the Ground field, H_G. To extract this profile, it was necessary to first determine H_{Pk}, which is defined as the amplitude of the modulation H_{Mod} during the transmitter "On" time. The next step was to apply corrections for the Primary field, $H_{Primary}$ and the Normal field, H_{Normal}. The amplitude of the so-corrected modulation is termed the Normalised TFMMR, H_N.

The amplitude of the fundamental frequency of a square wave is known from theory to be $4/\pi$ times the amplitude of the square wave (Eqn 5-1). Consequently, H_{Pk} was determined by dividing the more readily determined amplitude of the fundamental frequency by $4/\pi$. Calculation of H_{Pk} by this means has the additional advantage in that it is relatively immune to the influence of mains power noise. However, it was moderately affected in areas where the "spikes" described in Section 5.3 were present as a distortion of the H_{Mod} waveforms. Those situations were most significant where polarity reversals occurred in the profiles and resulted in some error in detecting the actual point of reversal. Otherwise, the error inherent in the method used for the determination of H_{Pk} did not significantly affect data quality.

Examples of polarity reversals occur at several points along the profile as can be seen in Figure 5-5(C). Because of the lack of synchronisation between the TM-4 and the transmitter, it proved difficult to automatically detect the sign of the modulation about these reversals. Cross-correlation detection techniques were attempted for this purpose.

However, it was found to be more reliable and, consequently, more expedient to examine each of the individual traverses by eye and to adjust the polarity of the data manually. The raw TFMMR data thus obtained, are shown in Figure 5-6(A).

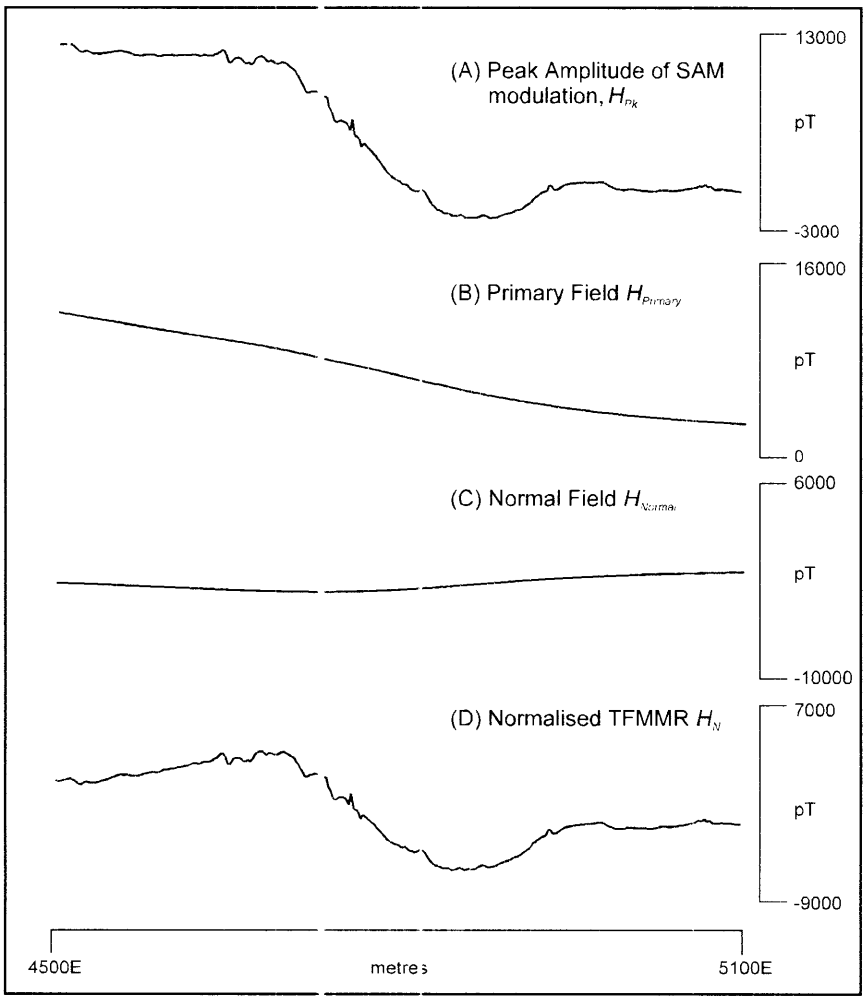

Figure 5-6. (A) Peak amplitude of the SAM modulation H_{Pk} determined from the data in Figure 5-5. (B) The calculated Primary Field $H_{Primary}$. (C) The calculated Normal Field H_{Normal}. (D) The Normalised TFMMR data H_N.

5.4.4 Correction for $H_{Primary}$ and H_{Normal}

The appropriate Primary and Normal fields were calculated for the known electrode and current-bearing wire locations and are shown in Figure 5-6(B) and Figure 5-6(C), respectively. Subtraction of both the Primary and Normal fields from the data in Figure 5-6(A) resulted in the data in Figure 5-6(D). In this case, the TFMMR anomaly is dipolar and centred approximately over the conductor which is located at 4800 mE and dipping a few degrees to the west.

5.4.5 Extraction of TFMMIP Parameters

An attempt was made to determine whether any IP information was evident in the data. Due to the lack of synchronisation between the transmitter and the TM-4 at the time of the survey, it was not possible to determine the phase angle between the observed magnetic field and the current applied to the ground. As an alternative, the spectral components of the waveform were examined.

The feasibility tests used a 100% duty cycle square wave as the transmitted signal. The square wave may be represented by a Fourier series which is a summation of the fundamental frequency and its harmonics. The Fourier series for a square wave of peak amplitude A_P and frequency ω is given by:

$$A = \frac{4A_P}{\pi}\left(\sin\omega t + \tfrac{1}{3}\sin 3\omega t + \tfrac{1}{5}\sin 5\omega t + \tfrac{1}{7}\sin 7\omega t \ldots\right) \qquad \text{Eqn 5-1}$$

The faithfulness of the series representation improves as the number of terms is increased. That is, the higher frequencies are necessary to reproduce the sharp corners of the square wave. A square wave has only real components and as indicated from Equation 5-1, only the odd harmonics of the fundamental frequency are present. As can be seen from the equation, the amplitudes of the harmonics are inversely proportional to the harmonic number.

The components of the square wave are illustrated by using the Fast Fourier Transform (FFT) to generate the frequency spectrum. The amplitude spectrum for a typical 1024 point section of the waveform in Figure 5-1 is shown in Figure 5-7. The amplitudes were normalised by dividing them by the amplitude of the fundamental frequency.

As can be seen from the figure, there are distinct peaks in the spectrum at the fundamental frequency (8 Hz) as well as the odd harmonics. All harmonics up to the 21st are clearly visible in the spectrum although those above the 13th have been inadequately sampled and appear as aliased frequencies. A peak at 50 Hz is due to mains power interference.

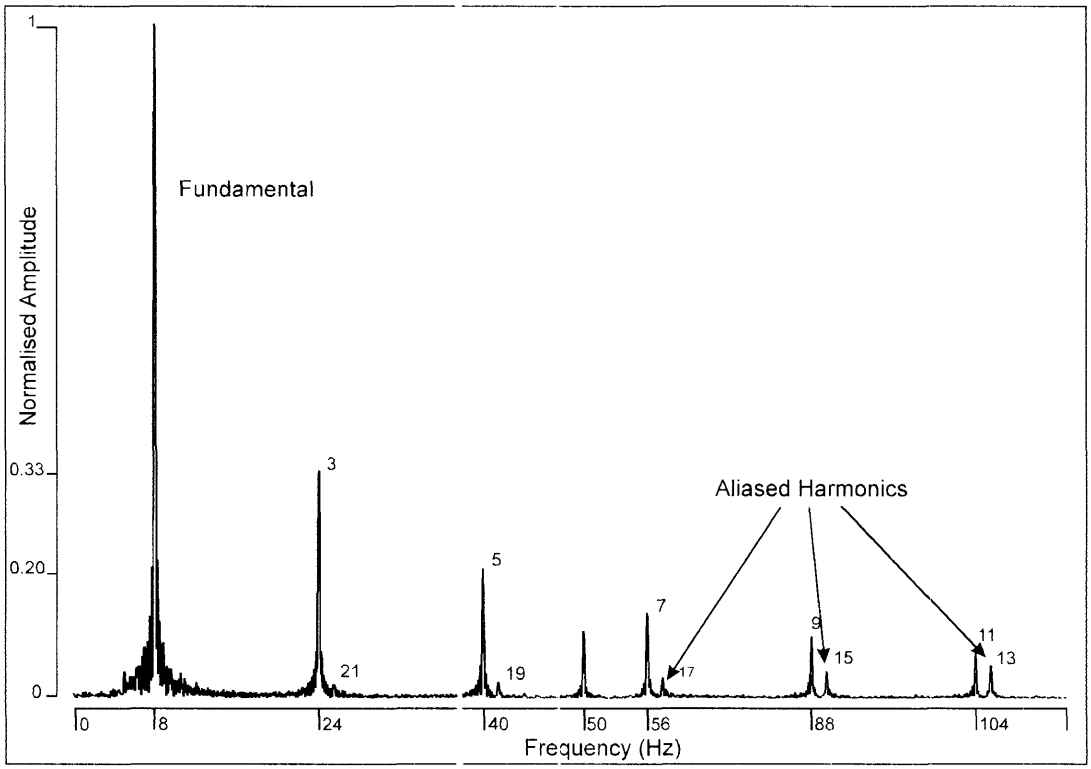

Figure 5-7. Normalised Amplitude spectrum of a 1024 point SAM signal showing the fundamental frequency and the odd harmonics. The harmonics above the 11th have been folded back about the Nyquist frequency due to aliasing.

Amplitude and phase relationships of the harmonics are often used as a measure of the IP response in conventional EIP and MIP surveys. These simple relationships are not entirely appropriate for TFMMIP data due to the influence of the Primary field. However, as a first attempt to determine whether any IP information was present in the data, the Relative Amplitude of the fundamental frequency and the 3rd harmonic were calculated for a running 1024 point window along the profile. The Relative Amplitude, RA, is defined by

$$RA = \frac{3 \times A_3}{A_1} \qquad \text{Eqn 5-2}$$

where A_1 and A_3 are the amplitudes of the fundamental and third harmonic, respectively.

The result of this exercise is shown in Figure 5-8. As can be seen from the figure, four distinct peaks resulted from this calculation. These peaks have been identified as

corresponding with the polarity reversals previously referred to, indicating that this technique is severely influenced by the degradation of the received signal due to the reduction in signal amplitude. The Relative Amplitude data was also found to be severely influenced by the effect of the Primary field. It was considered that this approach was not appropriate as a method for determining TFMMIP.

It became evident that any accurate investigation of IP parameters would not be possible using the data recorded during the feasibility trials due to the lack of precise synchronisation between the transmitter and the TM-4. Consequently, the major emphasis of the feasibility studies was constrained to an assessment of the validity and intrinsic value of the TFMMR parameter alone.

Figure 5-8. Relative amplitude of the 3rd harmonic and the fundamental frequency calculated from the data in Figure 5-5.

5.5 Data Quality

The data recorded during the feasibility trials were considered to be of high quality. Estimates of measurement resolution were made in areas relatively free from cultural interference and were found to be in the order of 0.05 nT which is the theoretical resolution for the TM-4 sampling rate used. The SAM signal, H_{Mod}, varied in amplitude up to about 20 nT in the survey areas although this was largely due to the Primary field. As a rule-of-thumb, the Ground signal, H_G, was characterised by amplitudes of up to

0.5 nT/A, resulting in signal-to-noise ratios of up to 50:1 (for typical transmitted currents of 5 A). As demonstrated by the Amplitude spectrum shown in Figure 5-7, the optically-pumped sensors were as far as could be determined with the available instrumentation, able to accurately track the rapidly varying magnetic field.

5.5.1 The Effect of High Frequency, High Amplitude Noise Resulting from the Spatially-varying Magnetic Field

Any degradation in the spatially-varying magnetic field, H_S, due to the electromagnetic modulation was not expected and was not observed in the processed data. However, extreme occurrences of high amplitude, high frequency variations in H_S may cause the Butterworth filter to "ring", resulting in the occasional corruption of the SAM waveforms. The result of this was that in magnetically "noisy" areas, typically up to 2% of the SAM data were deemed invalid. Bearing in mind the spatial density of the recorded data, this was considered an acceptable level of redundancy.

5.5.2 The Effect of EM Coupling

The similarity between the observed and synthetically modelled waveforms described in Section 5.3, provides supporting evidence that electromagnetic coupling and/or induced polarisation effects were present in the data from some of the survey areas. However, the technique described in Section 5.4.3 to determine the amplitude of the SAM modulation was found to be only moderately sensitive to these phenomena.

5.5.3 The Effect of Mains Power Interference

Power lines were present in several of the areas surveyed. In situations where surveys were conducted under major power transmission lines, the 50 Hz interference was observed to reach amplitudes of several thousand nanotesla. The optically-pumped sensor was able to track such modulation without difficulty. Although it was still possible to detect the SAM modulation, H_{SAMod}, within such noise, accurate determination of the amplitude of the signal proved more difficult.

The main reason for the difficulty was the TM-4's non-constant sample interval. Major fluctuations in the magnetic field due to the 50 Hz interference caused significant variation in the sample rate of the period counter during each cycle. That is, the high total magnetic field intensity encountered at the peak of the 50 Hz cycle resulted in a higher number of measurements being recorded than during the low field intensity phase of the cycle. As more data were recorded during the high field phase of the 50 Hz cycle than during the low field phase, the operation of the Butterworth filter introduced a systematic offset bias that could not be corrected.

The offset bias is significant when the amplitude of the 50 Hz interference exceeds several hundred nanotesla. In such situations, it is rare to find any geophysical method which is not affected by this interference. On the information available, the avoidance of a period counter in future SAM instrumentation will permit valid TFMMR data to be acquired even in such adverse conditions of interference.

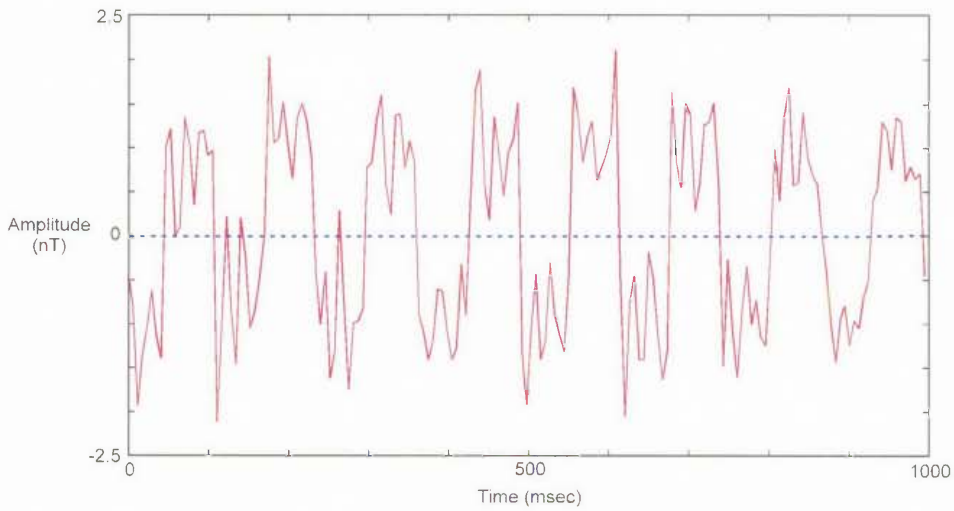

Figure 5-9. Recorded waveform showing 50 Hz mains power interference.

5.6 Discussion

The results of the waveform investigation suggested that the simultaneous acquisition of Total Magnetic Intensity (TMI) and Total Field Magnetometric Resistivity (TFMMR) was technically feasible. However, the feasibility of additionally acquiring Total Field Magnetometric Induced Polarisation (TFMMIP) information was not confirmed due to

deficiencies in the instrumentation used for the trials. The conclusions drawn from the study are summarised as follows:

- Spectral analysis of the recorded waveforms indicated that, as predicted from the manufacturer's specifications, the optically-pumped Cs vapour sensors used for the trials were capable of faithfully tracking the rapid oscillations in the magnetic field.
- The sample rate of about 200 Hz undersampled the higher harmonics of the transmitted frequency.
- Absolute instrument resolution (i.e. without signal enhancement) was of the order of 0.05 nT and was considered to be adequate for the measurement of TFMMR.
- The SAM signal levels ranged up to 20 nT, largely due to the Primary field ($H_{Primary}$) in areas nearest to the current carrying wire (generally about 200 m distant). Ground field signals (H_G) were characterised by amplitudes of up to 0.5 nT/A of current flow and were typically of the order of 5 nT.
- The H_S data were not noticeably degraded as a result of the processing required to remove the effects of the transmitted signal.
- The TFMMR data were adversely affected by high amplitude spikes in the spatially-varying magnetic field (H_S) which caused the Butterworth filter to "ring". These features were localised and resulted mainly from surface contamination in the test areas.
- Induced Polarisation and / or electromagnetic coupling was evident in the data. However, the instrumentation used for the trials proved to be deficient for the detailed investigation of these phenomena.
- Electromagnetic interference from mains power lines was observed at several sites. Filtering of the recorded signal to remove the high amplitude 50 Hz interference was found to be ineffective mainly as a result of the non-constant sample interval.
- Appropriate data reduction procedures were developed for the feasibility trials and, as far as could be determined, the data so extracted were consistent with expectations.

For the tasks required of a SAM receiver, several major deficiencies in the hardware were identified and are defined as follows:

(i). Inadequate bandwidth meant that the higher component frequencies of the received signal were undersampled.

(ii). The lack of synchronisation between the transmitter and the magnetometer prevented the automatic detection of polarity reversals and resulted in the inability to investigate IP or EM parameters.

(iii). The non-constant sample interval prevented the application of standard IP integration techniques or signal enhancement to the waveforms.